

A novel technique for mapping viscosity in discrete subcellular locations with a BODIPY based fluorescent probe

Lior Pytowski¹, Alex C. Foley¹, Zayra E. Hernández¹, Niall Moon², Tim Donohoe² and David J. Vaux^{1*}

¹ Sir William Dunn School of Pathology, University of Oxford, United Kingdom

² Department of Chemistry, University of Oxford, United Kingdom

* Author for correspondence (david.vaux@path.ox.ac.uk)

Abstract

Numerous cellular processes, including enzyme behaviour, signalling, and protein folding and transport are highly influenced by the local microviscosity environment within living cells. Molecular rotors are fluorescent molecules that respond to the viscosity of their environment through changes in both the intensity and lifetime of their fluorescence. We have synthesised a novel boron-dipyrrin (BODIPY) molecular rotor that is also a substrate for the SNAP-tag targeting system (named BG-BODIPY), allowing us to target the rotor to discrete locations within the living cell. We demonstrate that BG-BODIPY reports viscosity, and that this can be measured either through fluorescence lifetime or intensity ratiometric measurements. The relative microviscosities within the ER, Golgi, mitochondrial matrix, peroxisomes, lysosomes, cytoplasm, and nucleoplasm were significantly different. Additionally, this approach permitted fluorescence lifetime imaging microscopy (FLIM) to determine the absolute viscosity within both mitochondria and stress granules, showcasing BG-BODIPY's usefulness in studying both membrane bound and membraneless organelles. These results highlight targeted BG-BODIPY's broad usefulness for making measurements of cellular viscosity both with FLIM and conventional confocal microscopy, the latter option greatly extending the accessibility of the technique.

Keywords

Cellular microviscosity; molecular rotors; BODIPY; FLIM; TDP-43; stress granules; CRISPR

Introduction

Viscosity is an essential biophysical factor influencing numerous cellular processes for which diffusion has evolved to become the rate-limiting factor, such as signal transduction, protein-protein interactions, and intracellular transport of macromolecular cargo¹. Traditional methods of determining the viscosity of a substance by measuring its resistance to shear or tensile stress operate on continuous material at far too large scale to appreciate the microviscous environment within a cell. As we begin to understand that single cellular compartments may have significant local variations within them, and that our view of cellular compartmentalisation is lent further complexity by the presence of membraneless organelles, it becomes increasingly clear that we require a means of measuring viscosity at discrete locations in living cells².

Most attempts at measuring microviscosity in living cells have relied primarily upon a class of synthetic fluorescent molecules that respond to the local viscous environment, termed molecular rotors³. The viscosity-dependence of these fluorophores is mediated by the presence of a hinge domain in the probes that allows intramolecular rotation, creating competition for releasing the energy of an absorbed photon through either fluorescence or non-radiative decay via mechanical twisting of the molecule. Among this class of fluorophores, the most commonly

utilised are those which can access Twisted Intramolecular Charge Transfer (TICT) states, which are states of lower energy charge transfer resulting in decreased fluorescence emission intensity¹. The fluorescence intensity is directly influenced by the local viscosity, as an increase in viscosity will reduce the amount of intramolecular twisting, forcing the energy emission to occur through fluorescence, and vice versa. This results in both an increase in the fluorescence intensity and fluorescence lifetime of the molecule.

Boron-dipyrrin (BODIPY) is one of the most commonly used molecular rotors. Bodipy belongs to the TICT class of molecular rotors, and is therefore a viscosity reporter in that its de-excitation after absorbing a photon occurs through a competition between fluorescence and non-radiative decay through intramolecular rotation^{3,4}. BODIPY molecular rotors have a number of attractive traits, such as their strong UV absorbance, their stability in physiological conditions, and their tunability with small chemical modifications^{5,6}.

There has been a spate of efforts to map eukaryotic cells in terms of viscosity. Kuimova et al. (2008)⁴ loaded SK- OV-3c cells with *meso*-substituted 4,4'-difluoro-4-bora-3a,4a-diaza-s-indacene not conjugated to any targeting molecule, measuring the viscosity in various subcellular localisations. Levitt et al. (2009)⁶ used two *meso*-substituted BODIPY based fluors conjugated to hydrophobic groups designed to drive indiscriminate incorporation into the hydrophobic interior of non-aqueous cellular membranes, and discovered that the intracellular environment contains a wide range of viscosities. Several groups have targeted boron-dipyrrin (BODIPY) modified by the addition of triphenylphosphonium to target the dye to the mitochondria with varying degrees of success^{7,8}. More recently, Chambers et al. (2018)⁹, have developed a chloroalkane -BODIPY capable of targeting to specific organelles via a transiently expressed HALO-tag protein targeted to mitochondria or the ER lumen.

In parallel, our group has developed a method for targeting BODIPY conjugated via a linker moiety to a benzylguanine group to discrete cellular locations through SNAP-tag technology. SNAP-tag utilises an O⁶-alkylguanine-DNA alkyltransferase enzyme expressed either through transient expression or CRISPR knock-in. This modified enzyme binds a benzylguanine group to produce a covalent adduct that cannot be resolved, so that the enzyme becomes covalently linked to this substrate. Our method additionally benefits from the expression of an mCherry fluorophore, the SNAP-tag enzyme and the localisation signals, allowing us to map numerous cellular locations with a single BODIPY-based probe through both fluorescence lifetime imaging microscopy (FLIM) and ratiometric imaging.

In this paper we demonstrate that a novel SNAP-tag compatible BODIPY probe can be targeted to both membrane-bound subcellular compartments and membraneless organelles. We show that this new probe reports microviscosity in discrete cellular locations through both FLIM and ratiometric imaging when the BODIPY fluorophore is bound to a targeted SNAP-tag-mCherry fusion protein. This system presents many possibilities, as it can be combined with any number of target sequences or proteins, and can accommodate numerous sensors (for example for calcium ion concentration, pH, and redox potential)¹⁰⁻¹² so long as they can be conjugated to a benzylguanine group and exhibit cell-penetrant properties. Further, the ability to measure viscosity either by quantitating the intensity of the fluorophore signal or the variations of its lifetime confers upon this technique an improved degree of flexibility, with each complementary method exhibiting advantages over the other.

Results

BG-BODIPY, a novel molecular rotor, reports microviscosity in live cells in both the lifetime and intensity domains.

To measure microviscosity in discrete subcellular compartments, we created a viscosity sensor able to be targeted to multiple locations through a general mechanism. A novel BODIPY probe was synthesised to be used in conjunction with SNAP-tag technology, which we termed benzylguanine-BODIPY, or BG-BODIPY. The synthetic approach is fully described in Supplementary material. The probe comprised a BODIPY molecular rotor conjugated via a linker to a benzylguanine group, a substrate for the modified O⁶-alkylguanine-DNA alkyltransferase (AGT) employed by SNAP-tag, altered such that upon trying to cleave its substrate, the two become covalently linked¹³. We targeted BG-BODIPY in living cells with a high degree of specificity by expressing modified SNAP-tag as a fusion protein targeted to specific organelles.

In order to ensure that BG-BODIPY still responded to viscosity and that this response occurred over a useful and measurable range of lifetimes, we used an IsoCell microfluidics printer¹⁴ to create grids of 2 mm fluid cells, partitioned with a water-immiscible fluid (FC-40), and containing varying percentages (vol/vol) of glycerol (0 to 95%) and MOPS buffer at 7 different integer pH values (4 to 10). We found that the pH did not have a significant effect on either the measured lifetime or intensity of BG-BODIPY across the whole range of viscosities (Figure 1A, C). At each pH, we plotted the $\log \Phi_f$ against $\log \eta$ and determined that the ratio followed a linear relationship (Figure 1B).

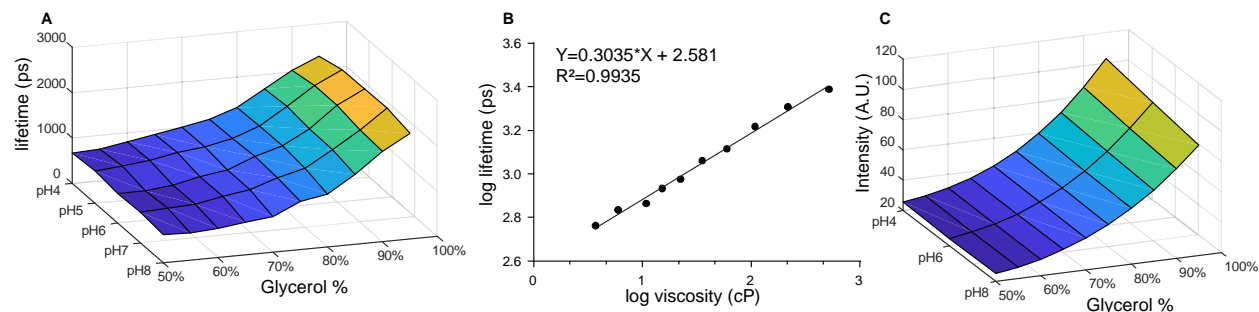


Figure 1: BG-BODIPY reports microviscosity in both the lifetime and intensity domains and is pH insensitive. Calibration of BG-BODIPY. **A.** The lifetime of BG-BODIPY in picoseconds (z axis) measured at various pH values (y axis) and glycerol concentrations (x axis). **B.** The log plot of fluorescence lifetime as a function of the log viscosity for BG-BODIPY in pH 7 MOPS buffer. The function is linear, expressed by the equation $Y=(0.3035)X+2.581$. **C.** The intensity of BG-BODIPY fluorescence measured at various pH values (y axis) and glycerol concentrations (x axis).

BG-BODIPY can be targeted to discrete membrane-bound organelles.

In order to target the BG-BODIPY to specific organelles, we expressed SNAP-tag fusion proteins either through transient transfection or using CRISPR-Cas9 to knock in the sequence into the AAVS1 safe harbour genomic locus in human cells. Initial experiments revealed significant non-specific dye retention after cell exposure, but this background could be eliminated by back-

extraction using three washes for 10 minutes with 5% delipidated bovine serum albumin (BSA) in DMEM as an absorber for the excess probe (supplemental figure 1).

In order to demonstrate that neither the expression of the fusion protein nor the loading of the SNAP-tag moiety with BG-BODIPY caused cellular cytotoxicity we collected time-lapse images after labelling for each of the cell lines. We found that BG-BODIPY exposure and the back-extraction do not affect cell viability as cells continue to divide and behave normally (supplementary movie 1).

Once we had a means of extracting the untargeted BG-BODIPY, we compared the colocalisation of Mitotracker with BG-BODIPY stained cells expressing a transiently transfected Cytochrome c oxidase 8A (Cox8) SNAP-tag fusion protein, or stably expressing a SNAP-tag fusion with mCherry and a mitochondrial targeting sequence after CRISPR/Cas-9 knock in of the appropriate construct to the AAVS1 safe harbour locus. We observed significant overlap of the BG-BODIPY and Mitotracker signals for both the CRISPR cell lines and the transiently transfected cells (Figure 2 A and B).

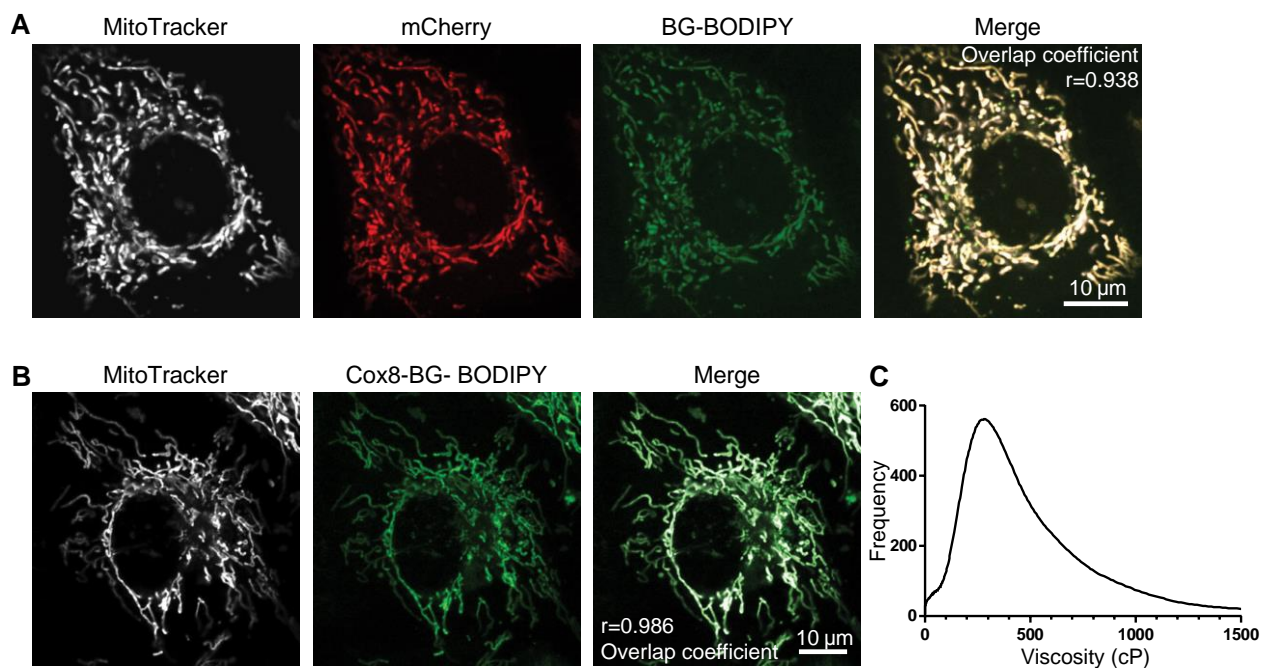


Figure 2. BG-BODIPY targets specifically to subcellular compartments. Colocalization of Mitotracker with **A.** mCherry and BG-BODIPY targeted to the mitochondria via residues 1 to 29 of HsCOX8 (Overlap Coefficient=0.938 $r^2=0.879$) and **B.** transient expression of a Cox8-SNAP-tag fusion protein (Overlap Coefficient=0.986 $r^2= 0.971$). **C.** Histogram of the viscosities reported from FLIM analysis of BG-BODIPY bound to the Cox8/SNAP-tag fusion protein. Mean viscosity 309 cP.

mCherry-BG-BODIPY can be targeted to selected cellular compartments and reports relative microviscosity.

To demonstrate the usefulness of BG-BODIPY in mapping viscosity throughout the cell, we measured the ratio of BG-BODIPY to mCherry fluorescence in all of the knock-in lines, which targeted the SNAP-tag enzyme to the endoplasmic reticulum (ER), the Golgi apparatus,

lysosomes, peroxisomes, mitochondria, the nucleoplasm, and the cytoplasm. We observed reported viscosities that vary significantly between the various membrane-bound organelles. For instance, the mean ratio value increased from the ER (1.67) to the Golgi (1.76) ($p < 0.001$), but the range of the ratio values broadened considerably. The second highest mean ratio, after the Golgi, was in the mitochondrial matrix (1.70). The lowest of the viscosities reported was in the nucleoplasm (1.45) which was significantly lower than the cytoplasm (1.56) ($p < 0.001$). Lysosomes had a mean lifetime slightly less than that of the cytoplasm (1.52), while peroxisomes had an intermediate mean lifetime (1.62), but exhibited by far the largest variance.

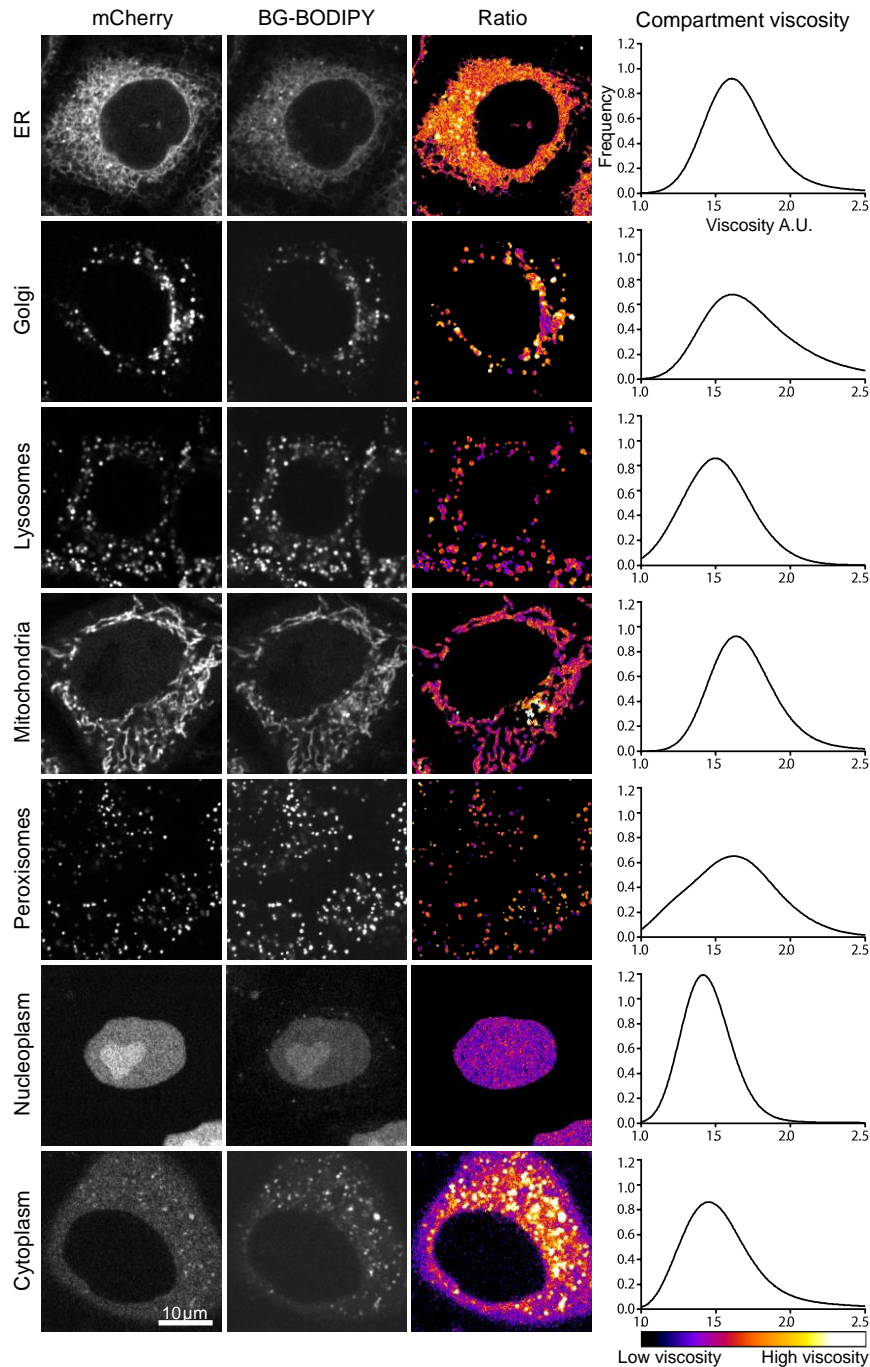


Figure 3: mCherry-BG-BODIPY can be targeted to all cellular compartments and reports relative microviscosity. The viscosity is highly variable in different cellular compartments. The mCherry-SNAP-tag fusion protein targeted to distinct cellular compartments was constitutively expressed from the AAVS1 locus and tagged with BG-BODIPY by subsequent incubation with the probe. Ratiometric analysis of the fluorescence intensity of mCherry and BODIPY enabled us to assess the compartment viscosity. The analysis shown is based on 3 experimental replicates of approximately 40 to 50 cells each.

BG-BODIPY can be targeted to measure viscosity in membraneless organelles.

To test whether BG-BODIPY could be used to probe cellular compartments formed through liquid-liquid phase separation, we expressed in HeLa cells a construct containing SNAP-tag fused to a C-terminal fragment of the TAR DNA-binding protein 43 (TDP-43) that lacks the RRM domains and is not itself prone to aggregation in physiological circumstances. TDP-43 is a constituent protein of the ubiquitinated inclusions observed in Amyotrophic Lateral Sclerosis (ALS) and frontotemporal dementia, and has been implicated in a number of other dementias, including Alzheimer's disease^{15,16}. Stress granules are cytoplasmic inclusions that sequester actively-translating mRNAs and distinct RNA binding proteins (RBPs) in conditions of oxidative stress. TDP-43 has been shown to associate with stress granules in a host of pathological conditions^{17,18}. ZnCl₂ has been shown to induce the formation of TDP-43 inclusions in the cytoplasm, and has been used to model pathological aggregation of the protein¹⁹. Therefore, we used ZnCl₂ to induce stress granules in HeLa cells expressing the TDP-43/SNAP-tag fusion protein²⁰.

When the lifetime of BG-BODIPY in the nucleus was measured by FLIM, we found the mean viscosity to be 185 cP (equivalent to the viscosity of 87.7% glycerol) (Figure 5), lower than that found in the mitochondria (309 cP) (Figure 2C). When cells were treated with 100 μ M ZnCl₂ overnight, a treatment shown robustly to elicit TDP-43 aggregation, we observed distinct populations of foci in the cytoplasm, demonstrating that the truncated TDP-43 is sequestered to stress granules upon oxidative stress (Figure 4AB). There was wide variation in the viscosities reported from within the stress granules, however we found that the mean viscosity was ~500 cP, a significant increase from TDP-43's nucleoplasmic microviscous environment.

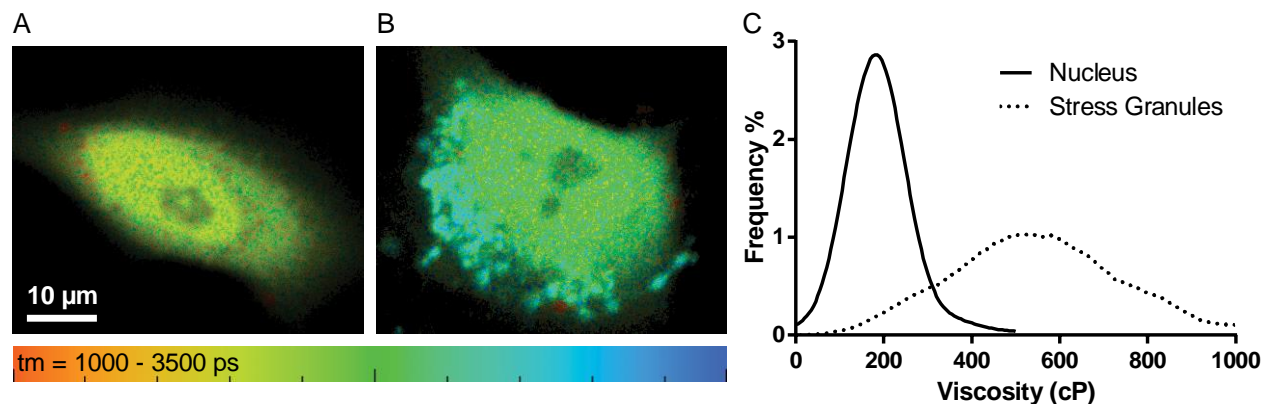


Figure 4: FLIM demonstrates that BG-BODIPY targets to and measures viscosity in membraneless organelles. **A.** C-terminal fragment of TDP43 labelled with BG-BODIPY targets to the nucleoplasm plus a diffuse cytoplasmic signal. **B.** In the presence of ZnCl₂ TDP43 forms

aggregates. **C.** the microviscosity within stress granules is significantly higher than that of either the nucleoplasm or cytoplasm.

Discussion

In this study, we demonstrated the usefulness of complementary techniques for measuring viscosity of discrete subcellular locations in living cells. Whilst numerous previous attempts to target molecular rotors in living cells have relied on exploiting the unique properties of given organelles^{7,8}, our work represents one of the first attempts at producing a generic mechanism to target BODIPY to any selected organelle or structure. We measured the relative viscosities of a host of organelles, as well as showcasing the BG-BODIPY's prospects for measuring absolute viscosity in both membrane-bound and membraneless organelles. We did so by CRISPR-Cas9 engineering the AAVS1 genomic locus in human cells to express the mCherry-SNAP-tag fusion protein targeted to multiple subcellular locations.

FLIM is a powerful technique that provides measurements of molecular rotor fluorescence lifetime, and thus absolute microviscosity, that are independent of probe concentration, but it has several practical limitations. Acquisition of FLIM images occurs over the order of minutes, with weaker signals requiring longer acquisition periods. This precludes the use of FLIM for capturing fast changes in viscosity. FLIM is also limited in most experimental systems to conventional confocal resolution, or at best two photon microscope resolution. This issue may be experimentally ameliorated by the selective targeting of the reporter via expression of organelle-specific fusion proteins bearing the SNAP-tag enzyme. Further, FLIM requires specialised, expensive equipment not available to most labs. In contrast, using BG-BODIPY with the ratiometric CRISPR cell lines allows us to visualise relative viscosity changes at higher spatial and temporal resolution, and can be measured using standard confocal microscopes. Thus, these two approaches represent complementary techniques that we offer together as additions to researchers' toolkits, each to be used situationally.

By using BG-BODIPY in these two methods, we were able to demonstrate its usefulness in probing the microviscous environments of the cell. We showed that there is significant variation in both the mean and the range of the viscosities seen within various cellular organelles. Of particular note is the change as one moves along the secretory pathway. Not only does the mean ratio between BG-BODIPY and mCherry increase from the ER to the Golgi apparatus, but there is also a progressively wider range of viscosities reported as one proceeds along the secretory pathway. We interpret this to mean that the microviscous environment becomes more varied later in the secretory pathway. Whilst the cause of this viscosity variation within an organelle later in the secretory pathway is unclear, it is tempting to consider whether this may be related to the formation of subdomains within later secretory organelles that facilitate separation of cargo with different destinations (secretory granule, constitutive secretion, shuttle vesicle to endocytic pathway).

Our measured viscosity ratios were comparable with those of Chambers et al. (2018)⁹, with the mitochondria having significantly higher mean viscosity than all organelles other than the Golgi apparatus, which they did not measure. Using FLIM we were able to determine that the absolute viscosity within the mitochondrial lumen was 309 cP. Chambers et al. (2018)⁹ found the viscosity within the mitochondrial lumen to be 325 cP, so our viscosity values are concordant, highlighting the replicability of this technique. However, our viscosity ratios in the cytoplasm and

nucleoplasm were not in concurrence with their measurements, as our probe reported a lower viscosity in the nucleoplasm than the cytoplasm, which may be due to cell type differences. Furthermore, the volume of distribution of the probes may not be comparable since previous attempts have relied upon an untargeted probe that was allowed to spread throughout the cell, whereas our probe was targeted to the nucleus or cytoplasm via either an NLS or and NES, respectively.

Beyond membrane-bound organelles, we demonstrate the possibility of microviscosity measurement within membraneless organelles by targeting BG-BODIPY to proteins involved in forming these organelles. We chose to examine TDP-43 positive stress granules because they represent a pathologically relevant instance of liquid-liquid phase separation. It is thought that the concentration of TDP-43 into stress granules can lead to aggregation of the protein, as seen in numerous neurodegenerative diseases¹⁷. The ability to measure the dynamic microviscosity environment of TDP-43 in a variety of physiological and disease conditions could lead to important discoveries in prevention of its cellular toxicity. What is more, by applying this technique to proteins involved in other membraneless organelles, we could gain key insight into the more general question of organisation of cellular space through phase separation.

In summary, the techniques presented here represent some powerful new tools for studying live cells. The CRISPR cell lines present a novel means of targeting SNAP-tag compatible probes to various cellular locations, without the disadvantages of transfection and transient overexpression. Any membrane-permeant probe compatible with SNAP-tag is compatible, and these cell lines could be just as easily used with Ca²⁺ or pH-sensing probes as they have been with BG-BODIPY. We have used both these cell lines, as well as transient transfection with SNAP-tag compatible constructs to demonstrate the potential for FLIM and ratiometric imaging of BG-BODIPY for the measurement of viscosity in living cells. These techniques allow a single probe to be adapted for use in a variety of circumstances, and allow viscosity measurements to be made by researchers without access to specialised FLIM equipment. The results presented here represent a small sample of the potential utility of the method, pose many questions about the role of viscosity in cellular processes, and facilitate wide-ranging future work in this area.

Materials and methods

Cell culture

HeLa cells were cultured in Dulbecco's Modified Eagle's Medium (DMEM) with 10% foetal bovine serum (FBS), 1% non-essential amino acids, and penicillin and streptomycin (100 units/ml). Cells were incubated at 37°C with 5% CO₂ in a humid atmosphere. For FLIM and confocal imaging cells were plated the day before, or three days prior to in the case of transfection, imaging on optical bottomed 96-well plates (PerkinElmer).

Generation of cell lines by CRISPR/Cas9

Donor plasmid generation

mCherry-SNAP-tag with the appropriate localisation signals and bGH poly(A) signal was inserted in the AAVS1 locus (GenBank accession AC010327.8 (7774 - 11429)) using a double-nicking strategy with the Cas9 D10A nickase mutant. The donor plasmid consisted of the insert enclosed

in a 840 bp C term homology arm GenBank accession AC010327.8 (8372 - 9211) and a 809 bp N term homology arm GenBank accession AC010327.8 (9212 - 10021) between position 70 and 71 of the lacZa gene of pBluescript. The donor plasmids were assembled by isothermal assembly (NEBuilder® HiFi DNA Assembly).

Localisations signals

Localisation signals were based on the protein localization signals database LocSigDB²¹ and Chertkova et al. 2017 findings²².

Table 1: Cellular localisation and respective localisation signals.

Cellular localisation	Localisation signal	Terminus
Nucleoplasm	Residue 126 to 132 of SV40 large T-antigen, 3 times: PKKKRKVDPKKRKVDPKKRKV	C-terminus
Cytoplasm	Consensus MAPKK-NES: NLVDLQKKLEELDEQQ	C-terminus
Peroxisomes	SKL	C-terminus
Endoplasmic reticulum	Residues 1 to 17 of Calreticulin precursor: MLLSVPLLLGLLGLAVA	N-terminus
	KDEL	C-terminus
Lysosomes	Residues 1 to 26 of HsLAMP1: MAAPGARRPLLLLLLAGLAHSAPALF	N-terminus
	Residues 27 to 407 of HsLAMP1: EVKDNGTACIMASFSASFLTTYEAGHVSKVSNMTPASAEVLKNSSS CGEKNASEPTLAITFGEGLYLLKLTFTKNTRYSVQHMYFTYNLSDTQFF PNASSKGPDTVSTTDIKADINKTYRCVSDIRVYMKNVTIVLWDATIQAY LPSSNFSKEETRCQDQPSPTTGPPSPPLVPTNPSVSKYNVTGDNG TCLLASMALQLNITYMKKDNTTVTRAFNINPSDKYSGTCGAQLVTLKVG NKSRVLELQFGMNATSSFLQGVQLNMTLPDAIEPTFSTSNYSKALQ ASVGNYSKCNSEEHIFVSKALALNVFSVQVQAFRVESDRFGSVEECVQ DGNMMLPIAVGGALAGLVLIVLIAYLIGRKRSHAGYQTI	C-terminus
Mitochondria	Residues 1 to 29 of HsCOX8, 4 times: MSVLTPLLLRGLTGSARRLPVPRAKIHSLGDPMSVLTPLLLRGLTGSAR RLPVPRAKIHSLGKLSVLTPLLLRGLTGSARRLPVPRAKIHSLGDPMS VLTPLLLRGLTGSARRLPVPRAKIHSLG	N-terminus
Golgi apparatus	Residues 3131 to 3259 of HsGiantin: EPQQSFSEAQQQLCNTRQEVNELRKLEEEERDQRVAENALSVAAEEQI RRLEHSEWDSSRTPPIIGSCGTQEALLIDLTSNSCRTRSGVGWKRVL RSLCHSRTRVPLLAAYFLMIHVLLILCFTGHL	N-terminus

gRNA plasmid generation

gRNA and plasmid design were done following Ran et al. (2013)²³ recommendations.

Guides were designed with MIT design tool: <http://crispr.mit.edu/> and inserted into Addgene Plasmid #48141 pSpCas9n(BB)-2A-Puro (a gift from Feng Zhang). Guides RNA were 5'GTCCCTAGTGGCCCCACTGT3' and 5'GACAGAAAAGCCCCATCCTT3'.

Transfection and cell sorting

Plasmids containing the guides and donor templates were transfected in HeLa cells using Lipofectamine 2000 following manufacturer recommendations. Cells were then left to recover and to express the fusion protein for a week before proceeding with cell sorting. Cell sorting was done on a BD FACS Aria III run with the Diva software version 8.0.2. Positive cells were sorted if red fluorescence was 10^3 times brighter than control cells (excitation at 561nm 50mW, emission filter 610/20). Positive cells were cloned by single cell sorted in an optical 96-well plate containing preconditioned media and the expected localisation of the fusion protein was confirmed by confocal microscopy.

SNAP-tag labelling for FLIM and confocal microscopy

Plated cells were treated with 2.5 μ M BG-BODIPY for 60 minutes. Cells were then washed three times for 10 minutes with 5% delipidated BSA in DMEM in order to back extract the remaining free fluor. Following washing, cells were covered in Fluorobrite DMEM (ThermoFisher) media for imaging.

Fluorescence lifetime measurements

Fluorescence lifetime imaging microscopy (FLIM) was carried out on an Olympus FV 1000 with a Becker & Hickl SPC-150 Time-Correlated Single Photo Counting (TCSPC) module. A 488 nm laser pulsed at 80 MHz was used as an excitation source. Fluorescence decay measurements were collected using the Spcm software and analysed using the SPCImage software provided by Becker & Hickl. A two exponential decay model was used for fitting the curves, denoted by the equation (1):

$$I(t) = \sum_{i=1}^{\eta} a_i \exp\left(\frac{-t}{\tau_i}\right)$$

where $I(t)$ is the time-independent fluorescence intensity, τ is the lifetime, and a is the amplitude.

All images were acquired with a 60x objective to negate any polarization effects, as NA=1.4 oil-immersion microscope lenses are free of anisotropy²⁴. All measurements were performed at room temperature.

Following multiexponential fitting, the raw lifetime data for each pixel was exported to FIJI, where regions of interest were selected to create region specific lifetime histograms that were converted to cP using the equation $Y=(0.3035)X+2.581$.

Confocal microscopy

Samples were imaged on a Zeiss LSM880 with Airyscan using a Plan Apochromat 40x 1.3 NA oil immersion lens. For ratiometric imaging 16-bit images were acquired with Zen Black software. Channel registration was done using 0.1 μ m TetraSpeck™ Microspheres and images were corrected for translation, rotation and scaling.

Viscosity probe calibration

The Förster-Hoffman equation (2) characterizes the power-law relationship of quantum yield and viscosity:

$$\Phi_f = z\eta^\alpha$$

where z and α are constants and Φ_f is the fluorescence quantum yield. The fluorescent quantum yield, and the other main parameter of fluorescence, the fluorescence lifetime, are defined by (3)

$$\Phi_f = \frac{k_r}{k_r + k_{nr}} = k_r \tau_f$$

where k_r and k_{nr} are the radiative and non-radiative decay constants, respectively. It follows that a plot of $\log \Phi_f$ against $\log \eta$ yields a straight line with slope α ²⁵.

To determine the effects of pH and temperature on the BODIPY probes, we created a series of MOPS buffers with pH's that varied as integers from 4 to 10. These buffers were then each mixed with a series of glycerol volumes to create buffers ranging in viscosity ranging from 0% to 95% glycerol. These buffers with varying pH and glycerol concentration were pipetted into microfluidic chamber grids, as described below, by an IsoCell, along with unbound BG-BODIPY at a concentration of 2.5 μ M. The lifetime and intensity of BG-BODIPY in these chambers were then measured by FLIM.

Creation of the microfluidic chamber grids

An IsoCell printer¹⁴ was used to create 7 x 15 grids for the calibration of the BODIPY dyes. The bottom of a 60 mm tissue culture polystyrene dish (Corning) was covered with DMEM + 10% FBS and the excess media removed. This was overlaid with an immiscible liquid, FC-40 (Fluorinert™). At the microscale, gravitational and buoyant effects become negligible and the interfacial forces pin the aqueous phase under the FC-40 to the plastic of the dish. The hydrophobic stylus with a conical tip made of polytetrafluoroethylene (Teflon) of the IsoCell printer was then lowered through both liquids until it makes contact with the dish. FC-40 wets the Teflon tip better than water, and so as the stylus was dragged laterally, the DMEM was displaced by the FC-40, which becomes pinned to the surface of the dish. A grid with 1.9 mm x 1.9 mm chambers was drawn in such a fashion and the DMEM was then removed from each grid chamber, pipetted out by the IsoCell, and replaced with a mixture containing 2.5 μ M BODIPY and varying concentrations of glycerol (0 to 95%) and MOPS buffers with pHs ranging from 4 to 10.

References

1. López-Duarte, I., Vu, T. T., Izquierdo, M. A., Bull, J. A. & Kuimova, M. K. A molecular rotor for measuring viscosity in plasma membranes of live cells. *Chem. Commun.* **50**, 5282–5284 (2014).
2. Gomes, E. & Shorter, J. The molecular language of membraneless organelles. *J. Biol. Chem.* jbc.TM118.001192 (2018). doi:10.1074/jbc.TM118.001192
3. Haidekker, M. A. & Theodorakis, E. A. Molecular rotors—fluorescent biosensors for viscosity and flow. *Org. Biomol. Chem.* **5**, 1669–1678 (2007).
4. Kuimova, M. K., Yahioğlu, G., Levitt, J. A. & Suhling, K. Molecular Rotor Measures Viscosity of Live Cells via Fluorescence Lifetime Imaging. *J. Am. Chem. Soc.* **130**, 6672–6673 (2008).
5. Loudet, A. & Burgess, K. BODIPY Dyes and Their Derivatives: Syntheses and Spectroscopic Properties. *Chem. Rev.* **107**, 4891–4932 (2007).

6. Levitt, J. A. *et al.* Membrane-Bound Molecular Rotors Measure Viscosity in Live Cells via Fluorescence Lifetime Imaging. *J. Phys. Chem. C* **113**, 11634–11642 (2009).
7. Su, D., Teoh, C., Gao, N., Xu, Q.-H. & Chang, Y.-T. A Simple BODIPY-Based Viscosity Probe for Imaging of Cellular Viscosity in Live Cells. *Sensors* **16**, 1397 (2016).
8. Song, X., Li, N., Wang, C. & Xiao, Y. Targetable and fixable rotor for quantifying mitochondrial viscosity of living cells by fluorescence lifetime imaging. *J. Mater. Chem. B* **5**, 360–368 (2017).
9. Chambers, J. E. *et al.* An Optical Technique for Mapping Microviscosity Dynamics in Cellular Organelles. *ACS Nano* **12**, 4398–4407 (2018).
10. Martineau, M. *et al.* Semisynthetic fluorescent pH sensors for imaging exocytosis and endocytosis. *Nat. Commun.* **8**, (2017).
11. Ruggiu, A. A., Bannwarth, M. & Johnsson, K. Fura-2FF-based calcium indicator for protein labeling. *Org. Biomol. Chem.* **8**, 3398 (2010).
12. Bannwarth, M. *et al.* Indo-1 Derivatives for Local Calcium Sensing. *ACS Chem. Biol.* **4**, 179–190 (2009).
13. Keppler, A. *et al.* A general method for the covalent labeling of fusion proteins with small molecules in vivo. *Nat. Biotechnol.* **21**, 86–89 (2003).
14. Soitu, C. *et al.* Microfluidic chambers using fluid walls for cell biology. *Proc. Natl. Acad. Sci.* **115**, E5926–E5933 (2018).
15. Neumann, M. *et al.* Ubiquitinated TDP-43 in Frontotemporal Lobar Degeneration and Amyotrophic Lateral Sclerosis. *Science* **314**, 130–133 (2006).
16. Arai, T. *et al.* TDP-43 is a component of ubiquitin-positive tau-negative inclusions in frontotemporal lobar degeneration and amyotrophic lateral sclerosis. *Biochem. Biophys. Res. Commun.* **351**, 602–611 (2006).
17. Parker, S. J. *et al.* Endogenous TDP-43 localized to stress granules can subsequently form protein aggregates. *Neurochem. Int.* **60**, 415–424 (2012).
18. Liu-Yesucevitz, L. *et al.* Tar DNA Binding Protein-43 (TDP-43) Associates with Stress Granules: Analysis of Cultured Cells and Pathological Brain Tissue. *PLoS ONE* **5**, e13250 (2010).
19. Caragounis, A. *et al.* Zinc induces depletion and aggregation of endogenous TDP-43. *Free Radic. Biol. Med.* **48**, 1152–1161 (2010).
20. Yang, C. *et al.* The C-terminal TDP-43 fragments have a high aggregation propensity and harm neurons by a dominant-negative mechanism. *PLoS One* **5**, e15878 (2010).
21. Negi, S., Pandey, S., Srinivasan, S. M., Mohammed, A. & Guda, C. LocSigDB: a database of protein localization signals. *Database J. Biol. Databases Curation* **2015**, (2015).
22. Chertkova, A. O. *et al.* Robust and Bright Genetically Encoded Fluorescent Markers for Highlighting Structures and Compartments in Mammalian Cells. (2017). doi:10.1101/160374
23. Ran, F. A. *et al.* Genome engineering using the CRISPR-Cas9 system. *Nat. Protoc.* **8**, 2281–2308 (2013).
24. Becker, W. *Advanced Time-Correlated Single Photon Counting Techniques*. **81**, (Springer Berlin Heidelberg, 2005).
25. Kuimova, M. K. Mapping viscosity in cells using molecular rotors. *Phys. Chem. Chem. Phys.* *PCCP* **14**, 12671–12686 (2012).

Acknowledgments

Cristian Soitu for microfluidic chamber preparation. The Micron Oxford Advanced Bioimaging Unit (funded from Wellcome Trust Strategic Award 107457/Z/15/Z) for technical assistance, discussions and advice. Michal Maj from the Flow Cytometry Facility - Sir William Dunn School of Pathology for cell sorting.

Author contributions

L.P., A.C.F. and D.J.V. conceived and planned the experiments. A.C.F. carried out the FLIM experiments. L.P. carried out the other light microscopy experiments. L.P. and Z. E. H. created the CRISPR'd cell lines. N.M. synthesized the BG-BODIPY under T.D. direction. L.P, A.C.F. and D.J.V contributed to the interpretation of the results. A.C.F. took the lead in writing the manuscript with support from L.P. and D.J.V. All authors provided critical feedback and helped shape the research, analysis and manuscript.

Competing financial interests

Authors declare no conflicts of interest with the contents of this article.